Ahadian, Hamidreza; Sharifi Zamani, Elaheh; Phiri, Josphat; Maloney, Thaddeus

Fast dewatering of high nanocellulose content papers with in-situ generated cationic micro-nano bubbles

Published in:
Drying Technology

DOI:
10.1080/07373937.2021.1942898

Published: 01/08/2022

Document Version
Publisher's PDF, also known as Version of record

Drying Technology
An International Journal

ISSN: (Print) (Online) Journal homepage: https://www.tandfonline.com/loi/ldrt20

Fast dewatering of high nanocellulose content papers with in-situ generated cationic micro-nano bubbles

Hamidreza Ahadian, Elaheh Sharifi Zamani, Josphat Phiri & Thaddeus Maloney

To cite this article: Hamidreza Ahadian, Elaheh Sharifi Zamani, Josphat Phiri & Thaddeus Maloney (2021): Fast dewatering of high nanocellulose content papers with in-situ generated cationic micro-nano bubbles, Drying Technology, DOI: 10.1080/07373937.2021.1942898

To link to this article: https://doi.org/10.1080/07373937.2021.1942898

Published online: 20 Jul 2021.

DRYING TECHNOLOGY
https://doi.org/10.1080/07373937.2021.1942898

Fast dewatering of high nanocellulose content papers with in-situ generated cationic micro-nano bubbles

Hamidreza Ahadian, Elaheh Sharifi Zamani, Josphat Phiri, and Thaddeus Maloney

Department of Bioproducts and Biosystems, School of Chemical Engineering, Aalto University, Espoo, Finland

ABSTRACT

Herein, an innovative method to improve the dewatering of micro- and nanofibrillated cellulose (MNFC) containing furnishes is proposed. This method is based on fiber flotation in which cationic bubbles are injected into the furnish to separate fibers from liquid medium and accumulate them on the surface of the furnish. These cationic bubbles are generated by pressurizing a solution of Hexadecyltrimethylammonium chloride in deionized water in a dissolved air flotation (DAF) tank. The drainage properties of the furnishes with MNFC content from 0% to 25% were studied. With the help of the cationic bubbles, drainage rate of 0% and 15% MNFC furnish increased from 183 ml/s to 210 ml/s and 38 ml/s to 113 ml/s, respectively. The final couch solids content of these furnishes also increased from 16 wt% to 23 wt% and from 21 wt% to 24 wt%, respectively. Cationic bubbles flocculate MNFC fibers and increase retention. Sheets characteristics including morphology, permeability, mass distribution and surface profilometry were investigated. Cationic bubbles help structure fiber elements and improve the sheet formation.

ARTICLE HISTORY
Received 27 November 2020
Revised 19 March 2021
Accepted 9 June 2021

KEYWORDS
Nanocellulose; dewatering; nanobubbles; flotation; paper making

Introduction

In classical paper manufacturing, an efficient dewatering section is necessary for low energy consumption and high production rate. At the same time, product quality must be maintained.[1–3] One of the important research directions in paper manufacturing is toward the use of nanomaterials as furnish components. This includes a family of cellulosic materials called micro- and nanofibrillated cellulose (MNFC). MNFC is deconstructed cell wall fragments – usually fibrils and fibril aggregates, which are much smaller than the parent pulp fibers. The small size and high surface area of MNFC inhibit dewatering and give a range of processing problems on the paper machine.[4–7] MNFC gives the possibility to develop a new generation of natural fiber products with improved properties such as higher strength, lower permeability and roughness and improved formation.[4,5] This is largely because MNFC cross-dimensional is in the order of one-thousandth of macro fibers. However, utilization of MNFC in papermaking operations still requires new approaches to solve the dewatering properties inherent in these furnishes.[8] This is especially the case where MNFC exceeds 5% of the furnish components.[6,7] In this case, the dewatering is too slow to allow high speed manufacturing on conventional paper machines.[8]

A typical paper machine applies increasing levels of vacuum to a furnish, beginning with hydrofoils and moving to vacuum boxes. Through a combination of filtration and thickening mechanisms, the furnish is consolidated to a coherent wet web. It has been shown that the two main mechanisms that control vacuum dewatering are compression and displacement dewatering.[9–11] Vacuum compresses the wet web, while displacement dewatering occurs when the air flows through the wet web and drives the water out of interfiber voids.[9,11–18] The main limiting factors of dewatering are permeability, compressibility of the wet web and the surface tension of water. These properties are affected by factors such as basis weight, consistency, refining, temperature, fibers flocculation, fines content and vacuum level.[9,11,12,19]

One of the factors that inhibits dewatering, particularly in the early part of the forming section, is sheet

CONTACT Hamidreza Ahadian hamidreza.ahadian@aalto.fi; Thaddeus-Maloney thaddeus.maloney@aalto.fi Department of Bioproducts and Biosystems, School of Chemical Engineering, Aalto University, Espoo, Finland.

Table 1. Measured properties of pulp and MNFC.

	Properties					
Samples	WRV (g_{water}/g_{solid})	Zeta (mV)	Drainability (°SR)	Length weighted fiber length (mm)	Fines content (%)	Viscosity (mPa.s)
Pulp	1.58	−32	23	0.94	1.53	–
MNFC	5.95	−29	–	0.13	–	37.2

sealing. Sealing is a phenomenon where the first layer of fibers/fines laid on the fabric inhibits dewatering, either by plugging the wire channels or providing a dense layer with low permeability.[20,21] To prevent sealing, several measures can be taken. For example, short positive pressure pulses are used to disrupt the first layer and prevent sealing.[22] In addition, cationic and anionic polyelectrolytes and microparticles are normally used to bind the fines to the fiber surfaces;[23–26] thus, preventing blockage of waterways and improving permeability.[26–28]

Modern paper machines are designed to handle furnishes whose dewatering characteristics fall within a certain range, which limits the application of MNFC.[3,6,23] There are a number of different technologies being explored to solve this problem. One possibility is to optimize the usual wet end parameters such as pH, conductivity and polyelectrolyte type and concentration.[6,7,28–33] Another potential approach is to apply shear to the furnish just before or during dewatering. This can lower furnish viscosity and improve dewatering.[34,35] Hydrophobization of fibers has been shown to improve the dewatering efficiency.[36] Recently, one study indicated that optimizing the duration and frequency of vacuum pulses could improve dewatering of MNFC containing furnishes.[37] Another study showed that by using electro-assisted dewatering of a cellulose nanocrystal suspension, the solid content of the furnish could increase to 15.3 wt%.[38]

One interesting approach to dewatering of high MNFC suspensions is to replace the aqueous phase with a foam. During the last decade, foam forming has been extensively studied as an alternative method for the production of high MNFC content products with high bulk and strength properties, such as in Styrofoam replacements. [39–41] This approach has also shown very good dewatering properties; possibly due to reduced surface tension and the structuring effect of bubbles.[39,40,42]

Application of microbubbles, and more recently nanobubbles, in separation science has also gained a lot of interest.[43–45] Nanobubbles are nanoscopic separated spherical gaseous cavities dispersed in an aqueous medium. Nanobubbles size ranges from 200 nm to 1 µm while bubbles size in a foam often ranges between 20 µm and 100 µm. Nanobubbles have a high surface area to volume ratio and a negatively charged surface, which can be altered by the addition of surfactants. Because of these properties, they effectively adsorb onto charged tiny particles.[40,46,47] Nanobubbles generation methods are divided into two main approaches. The first approach is where nanobubbles are generated in a flowing gas-liquid mixture through a nozzle. For example, in cavitation chambers where there is a sudden strong pressure drop in the flow or in pressurized tanks in which, air-saturated liquid flows through a nozzle. In the second approach, gas is blown into quiescent liquid by electrolysis, ultrasound, chemical reaction or through a sintered membrane.[43,44,46,48,49]

In this study, cationic bubbles as dewatering aids are examined for MNFC containing furnishes. The generated bubbles are in three different size range. This idea has its origins in dissolved air flotation, which is commonly used to separate fine ink particles in paper mill deinking plants. We have also been encouraged by several studies showing that foam bubbles can be used to increase dewatering and improve paper properties in MNFC containing furnishes.[39,40,42] In this study, the cationic bubbles attach to the fibers surfaces and cause them to move upward and separate from the suspension. Consequently, a two-phase structure is formed which significantly improves the dewatering. This phenomenon works based on the electrostatic interaction of cationic bubbles and fibers, and the changes in buoyancy of the fibers.[45,50–52]

Materials and methods

Materials

A dried, bleached birch hardwood Kraft pulp (BHKP) was provided by a Finnish pulp mill. A cationic surfactant Hexadecyltrimethylammonium chloride was purchased from Sigma Aldrich.

Furnish preparation and measurements were performed at room temperature. Deionized water was used for all experiments.

The pulp in 4 wt% consistency was beaten in a Voith LR40 laboratory refiner at 25 Kwh/ton. It was then stored at 3.8 wt% consistency.

To produce MNFC, refined pulp at 2.4 wt% consistency was defibrillated in a high-pressure homogenizer

Table 2. Composition of six furnishes prepared for dewatering experiments.

Furnish	Pulp mass fraction (%)	MNFC mass fraction (%)
P-MNFC0%	100	0
P-MNFC5%	95	5
P-MNFC10%	90	10
P-MNFC15%	85	15
P-MNFC20%	80	20
P-MNFC25%	75	25

(Microfluidizer M-110P, Microfluidics Corp., MA, USA) under the operating pressure of 2000 bar for 4 passes.

The pulp and MNFC characteristics are shown in Table 1. The drainability of pulp was measured according to ISO 5267-1:1999. The fiber length and fines content were measured with Fiberlab (Metso Automation, Finland). The zeta potential was measured using a ZetaSizer Nano ZS instrument (Malvern Instruments, UK) at 0.1 wt% consistency.

The water retention value (WRV) of MNFC was measured according to the method developed by Maloney.[30] The viscosity was measured with a Brookfield viscometer DV2T-RV at 10 rpm and 1.5 wt% using a vane spindle V-73.[53]

Generation of cationic bubbles

The bubbles were generated in DI water by dissolved air flotation (DAF) method. In this method, air is dissolved into DI water at high pressure. Rapid depressurization causes the formation of small air bubbles in a range of sizes. A commercial DAF tank 510 TK Profiline from GLORIA House and Garden was used for the generation of the bubbles. After dissolving the cationic surfactant in DI at a concentration of 0.035 wt%, the tank was pressurized for 24 h at 6 bars before the experiments. The depressurizing flow rate estimated to be 6 mL/s was controlled by connecting a needle valve to the nozzle. The amount of surfactant used was equal to 0.1 g/g_{fiber} for each furnish.

Characterization of cationic bubbles

Two different methods for measuring bubble sizes were used. The nano scale bubbles were measured in a ZetaSizer Nano ZS with dynamic light scattering. Larger micro and macrobubbles were measured with light microscopy and the images were processed using ImageJ Fiji software.

The total air content was estimated by applying a 700 mbar vacuum for 2 min to the suspension and comparing the volume of liquid before and after vacuum treatment.

Dewatering measurements

Six furnishes of HBKP pulp and MNFC were prepared and their composition are shown in Table 2. The target grammage of each furnish was 100 g/m^2. The same furnish was used for both experiments with and without cationic bubbles. To prepare each furnish, the total required amount of pulp and MNFC were mixed, diluted to 2000 ml and disintegrated in a British L&W disintegrator for 12000 revolutions. It was then diluted to 0.13 wt%.

The dewatering experiments were performed in a modified Dynamic Drainage Analyzer (DDA 5, PulpEye, Sweden) with a 10 cm diameter etched screen with 50 µm conical holes (Gronmark, Finland). For the dewatering, a 300-mbar vacuum pressure was applied for 90 s. An ultrasonic level sensor on top of the DDA vessel measures the volume of the furnish during drainage.

For the experiments without cationic bubbles, 200 ml of DI water was added to a 600 mL furnish in the DDA vessel, mixed at 1000 rpm for 10 s, followed by a 20 s rest time before dewatering commenced.

For the experiments with cationic bubbles, 200 ml of air-saturated DI water was directly injected into 600 mL furnish while it was being mixed at 1000 rpm in the DDA vessel. In this case, the rest time was 2 min, which allowed the solid material to float to the surface (Figure 1). The thickness of each floated layer was recorded, and the concentration calculated. The amount of surfactant in each furnish was 0.1 g/g_{fiber}.

For both experiments with and without bubbles, 6 replicates were conducted. The furnish consistency was adjusted to 0.1 wt%.

Experiments were also carried out at different furnish concentrations in order to help elucidate the mechanism by which the bubbles improve dewatering. Six furnishes with the same compositions to the previous ones, but in different concentrations, were prepared. The concentration of each was equal to the calculated concentration of each floated layer. These measurements were conducted without the addition of bubbles.

Characterizations of samples

Three of the dewatered samples were dried at 105 °C to calculate retention and solids content. The other three sheets were freeze-dried in a vacuum chamber

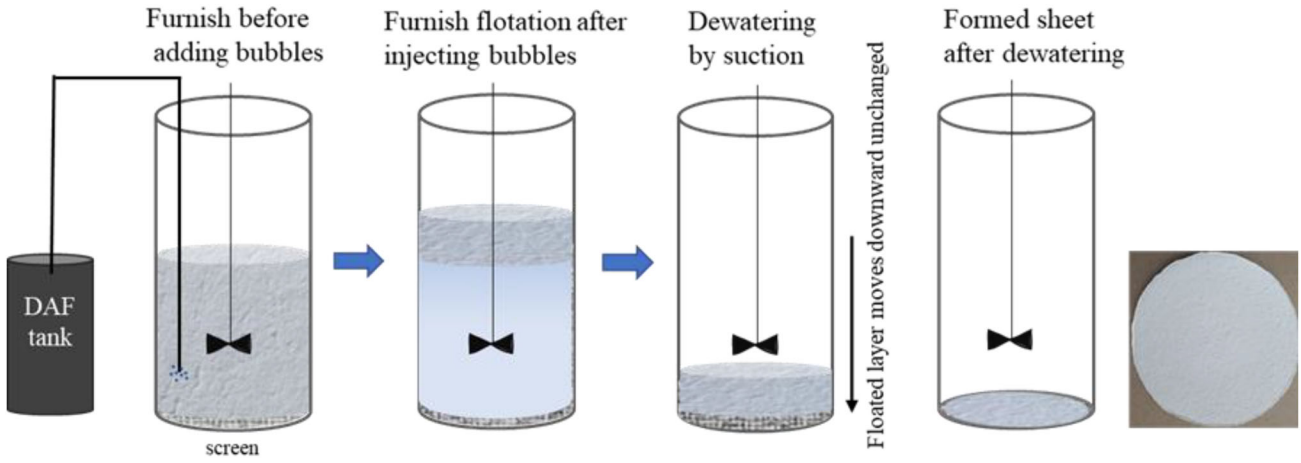

Figure 1. Schematic illustration of dewatering experiments with bubbles in the DDA.

at −40 °C and 0.4 mbar (Labconco Freezone 2.5, USA) to provide water dried samples for structural analysis. This was done to avoid the shrinkage and consolidation effects of water drying. The freeze-dried sheets were stored at a temperature of 23 °C and relative humidity of 50% according to standard ISO 187:1990. Neither the oven dried, nor the freeze-dried sheets were couched or pressed. The sheet properties were determined according to the following standards and devices: Bulk (ISO 534, L&W SE 250 D); air permeability (ISO 5636-3, Bendtsen, L&W SE 114); formation (SCAN-P 92:09, Beta radiation-based grammage formation, Ambertek); and topography (ISO 25178, L&W OptiTopo).

Empirical model for analyzing vacuum dewatering experiments

To deeply understand the dewatering mechanisms of the furnish with and without bubbles, an empirical mathematical model (Eq.1) of the normalized drainage curves is employed,

$$v = v_0 + v_{max}\left(1 - e^{-t/\tau}\right) + b.t \qquad (1)$$

where v is the normalized drained volume of the furnish, v_0 is the initial normalized volume, which is zero here, v_{max} is a factor corresponding to the maximum value of v, t is normalized time, τ is the time constant which is furnish dependent and corresponds to the viscous damping of the system, b indicates the effect of air displacement.[19,54]

Results and discussion

Cationic bubble characteristics

The average zeta potential of the bubbles was +45 mV. The generated bubbles were in three different groups of sizes (Figure 2). The first group of bubbles termed nanobubbles were in the range of 300–500 nm. The other groups termed microbubbles were in the range of 2–10 µm and macrobubbles around 50–90 µm. The calculated surface area to volume ratio of the nanobubbles, microbubbles and macrobubbles are around 10.02, 0.60, 0.04, respectively. As the surface area to volume ratio of nanobubbles is much higher than the surface area to volume ratio of microbubbles, nanobubbles are more effective in colloidal interactions between solids and cationic bubbles, for instance in flocculation of fibers. On the other hand, the microbubbles play a major role in the flotation and bulk variations of fibers network due to the higher volume fraction.

The air content was measured to be 5% (v/v), meaning that for each 200 ml of air-saturated water injected into each furnish, 10 mL was air. This value includes both dissolved and dispersed air content.

Fibers separation analysis

The separation of solid material is shown schematically in Figure 3. The cationic bubbles adsorb onto the anionic fibers surface. When the buoyancy force exceeds the gravitation force the fibers rise to the suspension surface.[52]

The equilibrium concentration of the separated surface layer depends on the amount of MNFC, as shown in Figure 4a,b. A higher MNFC content gives a lower concentration of the separated layer, presumably due to a structural organization of the cationic bubbles, fibers and fibrils in the separated layer (Figure 4c). This may have some positive effect on dewatering since lower packing of solid particles helps maintain high permeability and prevent sealing of the exit layer. The low solids content of the high MNFC sample is

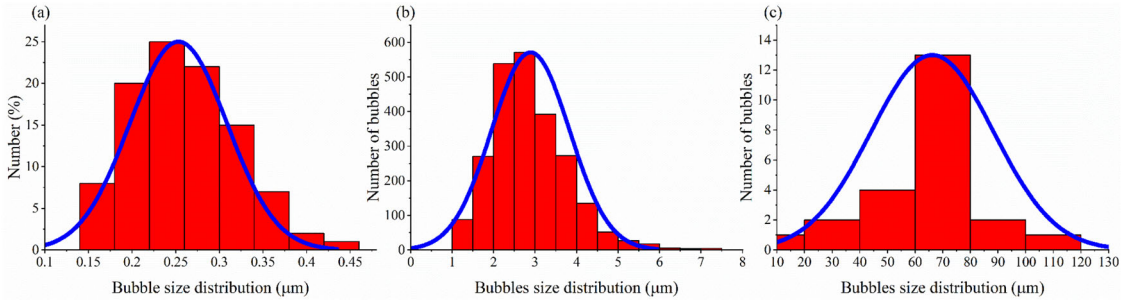

Figure 2. The size distribution of bubbles in the range (a) 0.1–1μm. (b) 1–10 μm and (c) 10–100 μm.

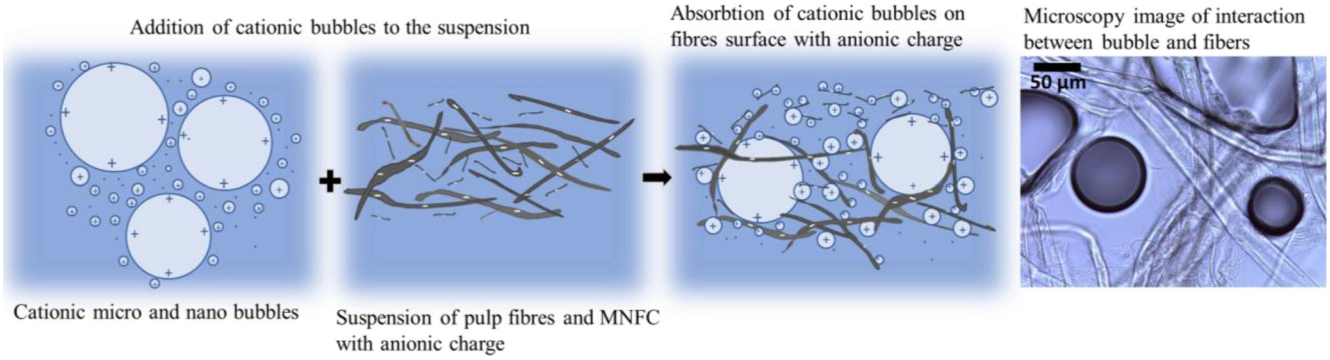

Figure 3. Interaction of fibers with cationic bubbles.

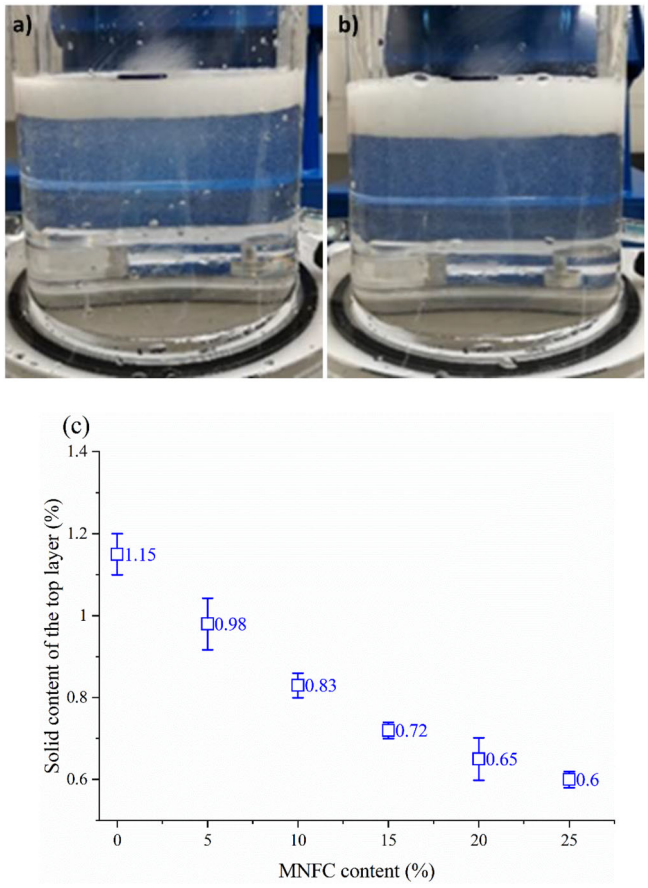

Figure 4. (a) P-MNFC5% after flotation. (b) P-MNFC20% after flotation. (c) Solids concentration of the top layer as function of MNFC content.

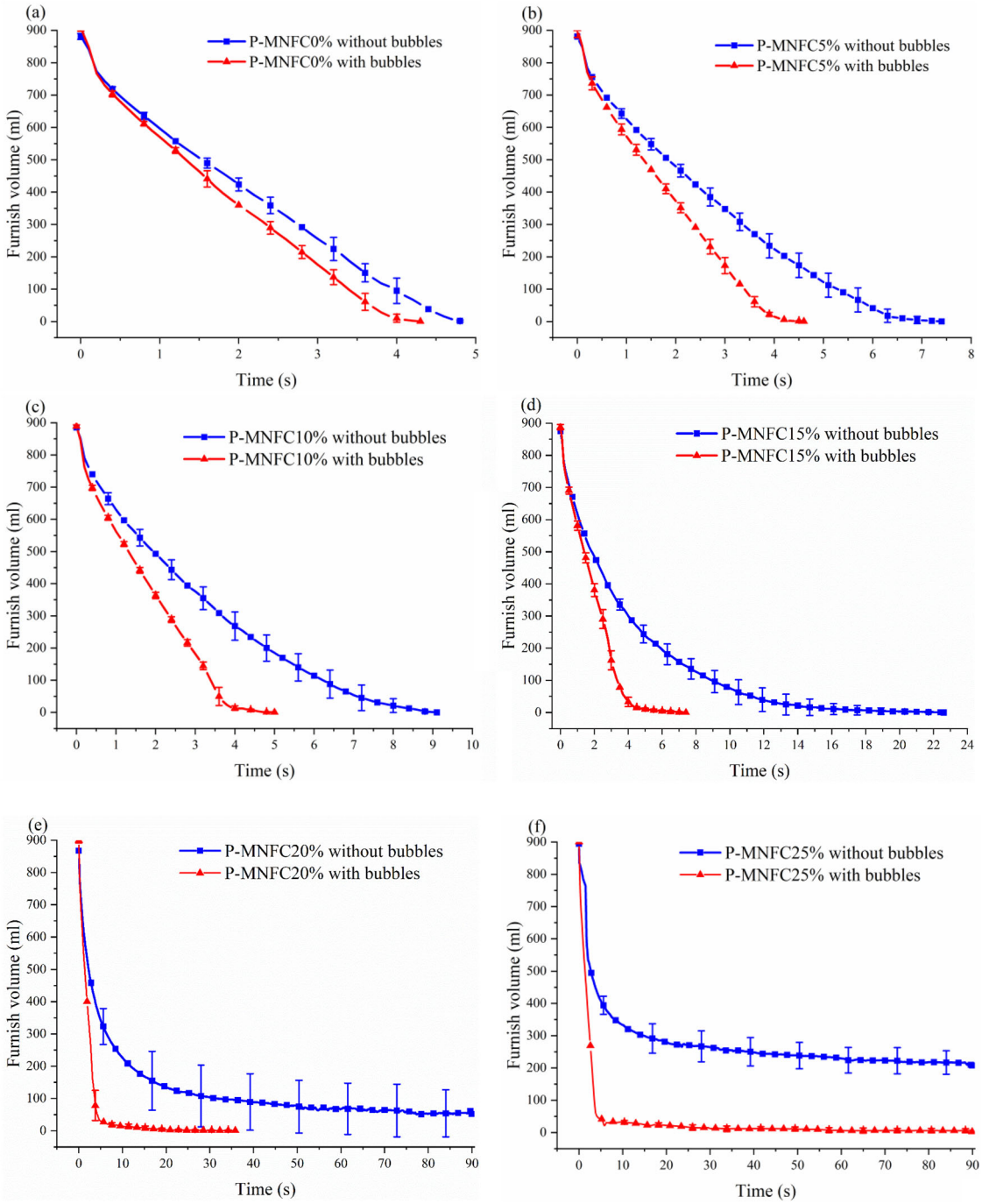

Figure 5. Furnish volume with and without bubbles during dewatering. (a) P-MNFC0%, (b) P-MNFC5%, (c) P-MNFC10%, (d) P-MNFC15%, (e) P-MNFC20% and (f) P-MNFC25%.

contrary to what is normally seen after consolidation and drying, where the density of the sheet usually increases with MNFC content.

Drainage properties

The drainage of the different furnishes was measured with the DDA in a classical 1-dimensional filtration experiment under steady state conditions, without pulsation. This differs from a paper machine where alternating vacuum and positive pressure pulses are used to dewater the furnish.[19,55] The curve of the furnish volume over time can be used to calculate the instantaneous drainage rate at any time from the initial conditions, until about what is referred to on the paper machine as "couch solids"; when air displacement no longer effectively displaces water and water removal effectively stops (Figure 5). Couch solids can be defined as the ratio of dry mass to the total mass of wet sheet after vacuum dewatering.

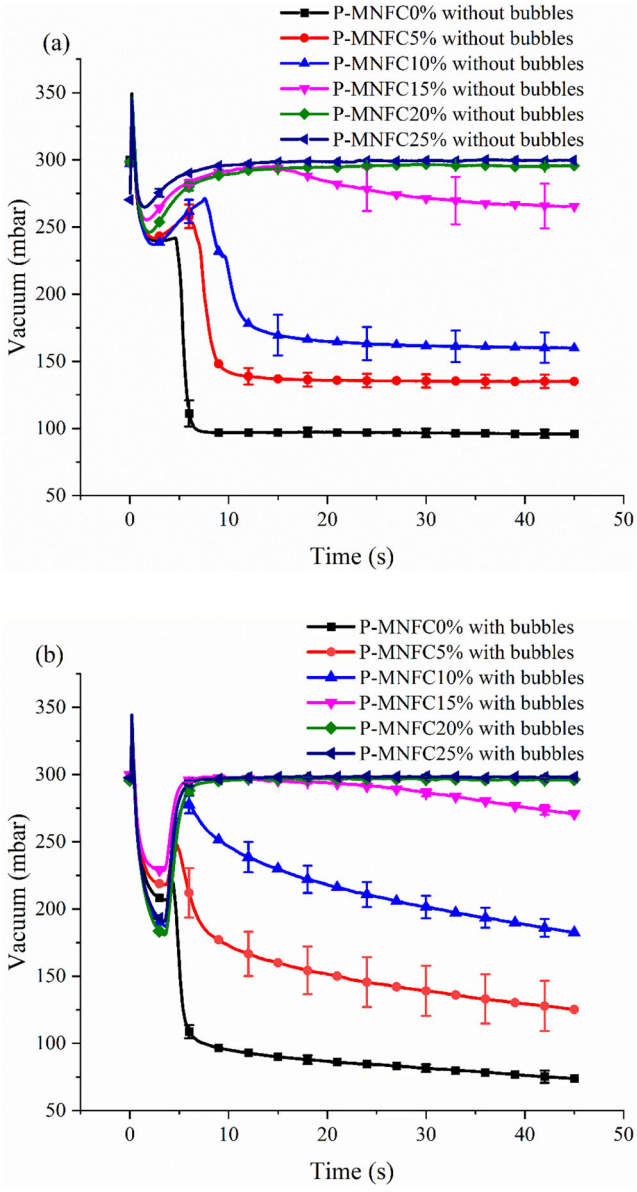

Figure 6. Vacuum curves as a function of time during dewatering of (a) Furnishes without bubbles and (b) Furnishes with bubbles.

A sample collected after dewatering (vacuum was applied 90 s in all experiments) can be used to evaluate the couch solids gravimetrically.

The DDA applies a constant vacuum load to the draining furnish with the aid of a vacuum pump until the free water is removed and air displacement commences. Depending on the dewatering rate and movement of air through the sheet, the actual pressure under the sheet varies. Thus, the vacuum level under the forming sheet gives indirect information on the dewatering stages, as shown in Figure 6. In particular, the sudden drop in the vacuum level corresponds to the point air enters the fiber network and the furnish changes from a two-phase system to a three-phase system. This corresponds to as the "dry line" on a paper machine. The vacuum level at the end of the experiment gives an indirect measure of the wet sheet permeability.[56]

It is clear that as the MNFC amount increases, the dewatering times also increases (Figure 5). At around 20 to 25% MNFC, a point is reached where the dewatering effectively stops – the sheet is completely sealed. This can be seen in Figure 5f where the furnish reaches a nearly constant volume of around 200–250 mL. Sheet sealing effectively limits the maximum amount of MNFC that can be used on a paper machine using the current technology.

Cationic bubbles were found to be a very effective dewatering aid over a range of MNFC content from 0 to 25%. This is shown by the faster dewatering times in Figure 5a–f. The addition of cationic bubbles to the furnish causes a phase separation and increases the concentration of solid material in the top layer. The removal of water in the lower phase offers essentially no dewatering resistance as shown in Figure 5. The solids content of the top layer is shown in Figure 4c. The solids contents of the top layer of furnishes after flotation is in the range of 0.6 to 1.3 wt% compared to the solids content of 0.1 wt% for the unseparated case. Higher solids content increases the dewatering efficiency since less water needs to be removed from the web. Moreover, there is less tendency for MNFC to enrich on the wire side, seal the sheet and inhibit dewatering. This can be clearly seen in Figure 5f (25% MNFC) in which the cationic bubbles containing furnishes dewaters in around 5 seconds, compared to the furnish without cationic bubbles which reaches a quasi-equilibrium and effectively stops dewatering with over 200 mL of furnish remaining. It is notable that the standard deviations of drain curves without bubbles are much bigger than drainage with bubbles. We believe that this is due to a higher variation in the z-direction distribution of fine particles in the web produced without bubbles. In cases where enough nanocellulose is enriched on the exit layer, the dewatering is severely inhibited. This is a well-known effect on industrial paper machines. In the case where cationic bubbles are applied, the consistency is effectively increased and the uniformity of fine particles throughout the web's z-direction is increased. This leads to more consistent dewatering results.

The shape of the vacuum curves in Figure 6 shows that for furnishes without or containing a small amount of MNFC, the vacuum drops and a dry line is established. In other words, air enters the sheet in the

Table 3. Empirical normalized dewatering parameters of the furnishes (the values are nondimensional).

	Normalized initial drain rate		Time constant, τ		R^2	
Samples	Without bubbles	With bubbles	Without bubbles	With bubbles	Without bubbles	With bubbles
P-MNFC0%	23.6	47.3	0.024	0.0030	0.97	0.99
P-MNFC5%	20.8	47.3	0.030	0.0037	0.98	0.99
P-MNFC10%	20.3	47.2	0.034	0.0037	0.99	0.99
P-MNFC15%	20.2	43.9	0.042	0.0073	0.99	0.99
P-MNFC20%	18.2	37.9	0.040	0.0110	0.96	0.90
P-MNFC25%	17.3	34.6	N/A	0.0100	N/A	0.90

later stages of dewatering and displaces water. Higher MNFC content increases the final vacuum level, showing these sheets have lower permeability, as expected. At around 15–20% MNFC, no clear drop in the vacuum curve is observed and the classical dry line is no longer formed. In these cases, dewatering essentially stops before air displacement begins. The shapes of the curves are somewhat different with and without cationic bubbles, but the pattern is similar in both cases.

We further investigated the dewatering mechanism of the furnishes by fitting the empirical model (Eq. 1) to the normalized data. After normalization of the dewatering curves by initial volume, the final fitted equation is:

$$v = \frac{(1-b)}{(1-e^{-1/\tau})}(1-e^{-t/\tau}) + b.t \qquad (2)$$

The first part of the model describes the viscoelastic behavior of the furnish under vacuum and the second linear part represent air displacement.[19,54] Table 3 shows some analytical parameters which have been extracted from the normalized volume curves in Figure 7. To compare the sheet sealing of two different furnishes, the initial drainage rate was calculated for the first two seconds. The initial drainage rate of furnishes without bubbles is almost half the initial drainage rate of the separated layer with bubbles. This indicates the reduction of sheet sealing by the addition of cationic bubbles. Moreover, fitting the Eq. (2) to the normalized curves yields the time constant τ, which is shown in Table 3. τ is the viscous damping which gives an indication of sheet sealing,[19,54] and is direct proportional to the amount of MNFC, supporting the notion that MNFC leads to high sheet sealing. However, when bubbles are introduced into the system, τ is significantly reduced. The R^2 is a statistical measure evaluating the goodness of fitting. The better a model fits the data, the closer the value of R^2 is to 1.[57]

The cationic bubbles are not just acting in a flotation capacity but have other effects that influence the dewatering. The cationic bubbles will attach to the anionic fibers and flocculate the MNFC. Both bubbles (as in foam forming) and cationic particles (in classical papermaking) have pronounced effects on improving the dewatering of fiber furnishes. In the current study, there is a hybrid system in which the bubbles separate, flocculate and structure the MNFC and fiber elements. The net effect on couch solids can be seen in Figure 8a. For the furnish without bubbles, the couch solids increase from 16% to about 20% at about 15% MNFC content then decreases significantly. There is a maximum in this curve because reducing sheet permeability increases sheet compression and water displacement under vacuum up to a point. When the sheet becomes sufficiently impermeable, air no longer overcomes the surface tension of water in the interfiber pores to displace the water. In Figure 8b the experiment is repeated without bubbles by using the same solids content as in a separated layer (Figure 4). The maximum in the couch solids curve is still observed, but the overall couch solids is around 20% compared to the value of 24% when cationic bubbles are used. There appears to be a significant positive effect of component structuring and surface tension effects on couch solids when cationic bubbles are used. The increase in the consistency of the separated layer does not explain this effect. Regardless of the furnish consistency or the use of cationic bubbles, the results indicate that addition of moderate amounts of MNFC can increase the couch solids, helping to improve overall paper machine dewatering efficiency.

The cationic bubbles were also found to have a profound effect on retention. Hydrodynamic shear and turbulence in the forming section can easily wash the relatively small MNFC particles from the web and reduce retention. Figure 9a reveals that for the furnish without bubbles, the retention decreases with increasing MNFC, however, for the furnish with bubbles, the retention remains almost constant. This is due to the flocculation of anionic particles to the cationic bubble surface, preventing them from washing through the web.[58,59] Increased consistency can also improve retention, but in this case, Figure 9b indicates consistency has a negligible impact. The improvement in retention appears to be related to charge neutralization and aggregation effects of the bubbles.

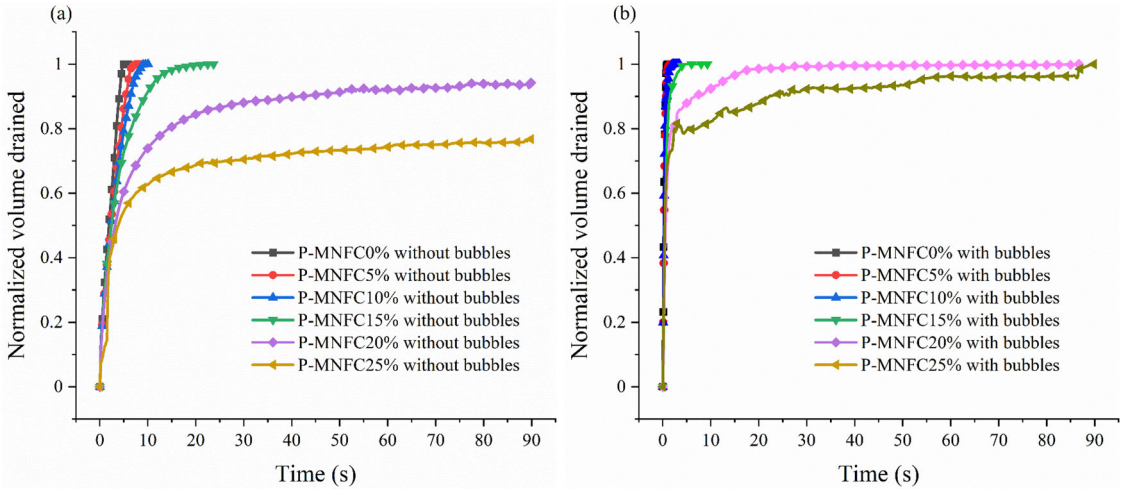

Figure 7. Normalized volume which is drained. (a) Furnishes without bubbles. (b) Furnishes with bubbles.

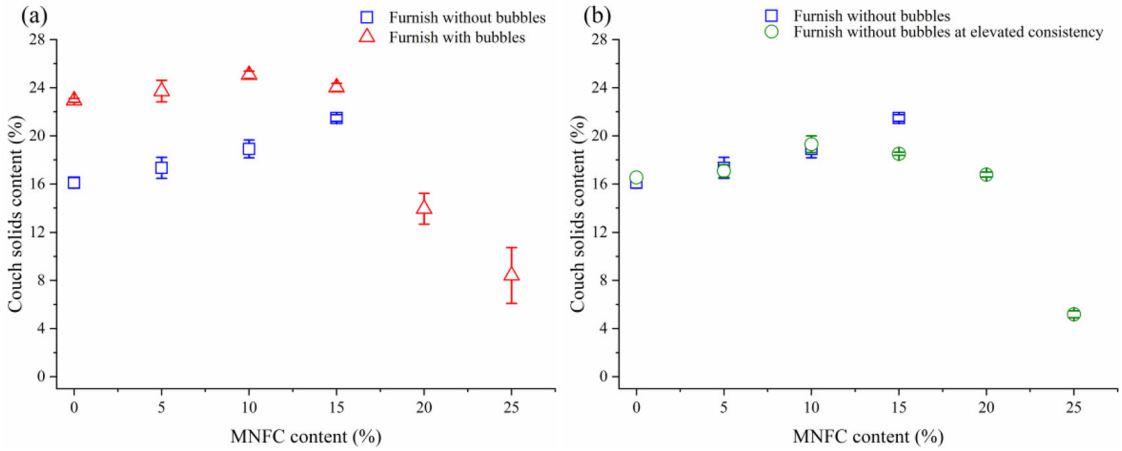

Figure 8. Couch solids content. (a) Furnish with bubbles vs without bubbles. (b) Furnish in high consistency vs without bubbles, the consistency of the green points are: 0% MNFC = 1.15 wt%, 5% MNFC = 0.98 wt%, 10%MNFC = 0.83 wt%, 15%MNFC = 0.72 wt%, 20%MNFC = 0.65 wt%, 25%MNFC = 0.6 wt%.

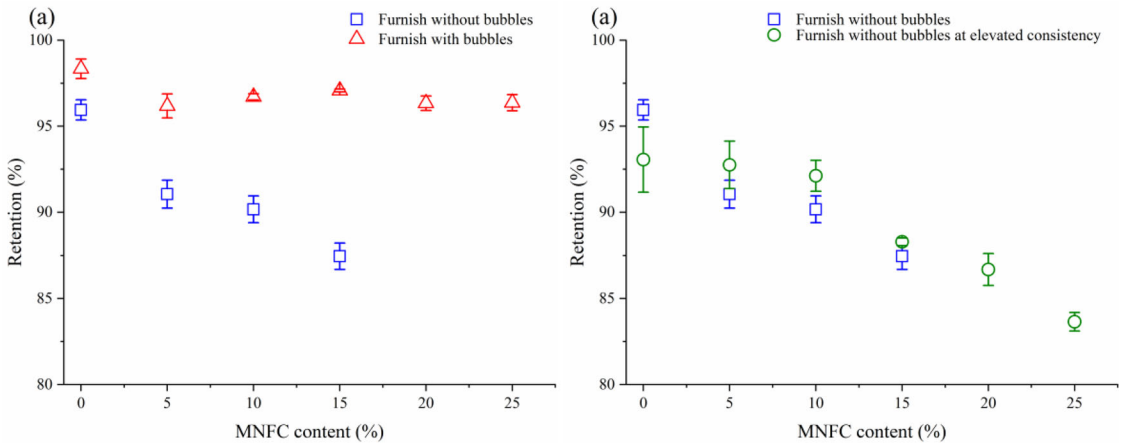

Figure 9. Retention. (a) Furnish without bubbles vs with bubbles. (b) Furnish without bubble vs furnish at elevated consistency.

In Figure 10, the SEM images of the wire side show less MNFC on the exit layer of the sheets with cationic bubbles. This reduces sheet sealing thus improves dewatering. On the other hand, the SEM images of the top sides in Figure 11d shows an enriched layer of MNFC for the sheets with bubbles which is clearly greater than for the sheets produced without bubbles in Figure 11b. This indicates that

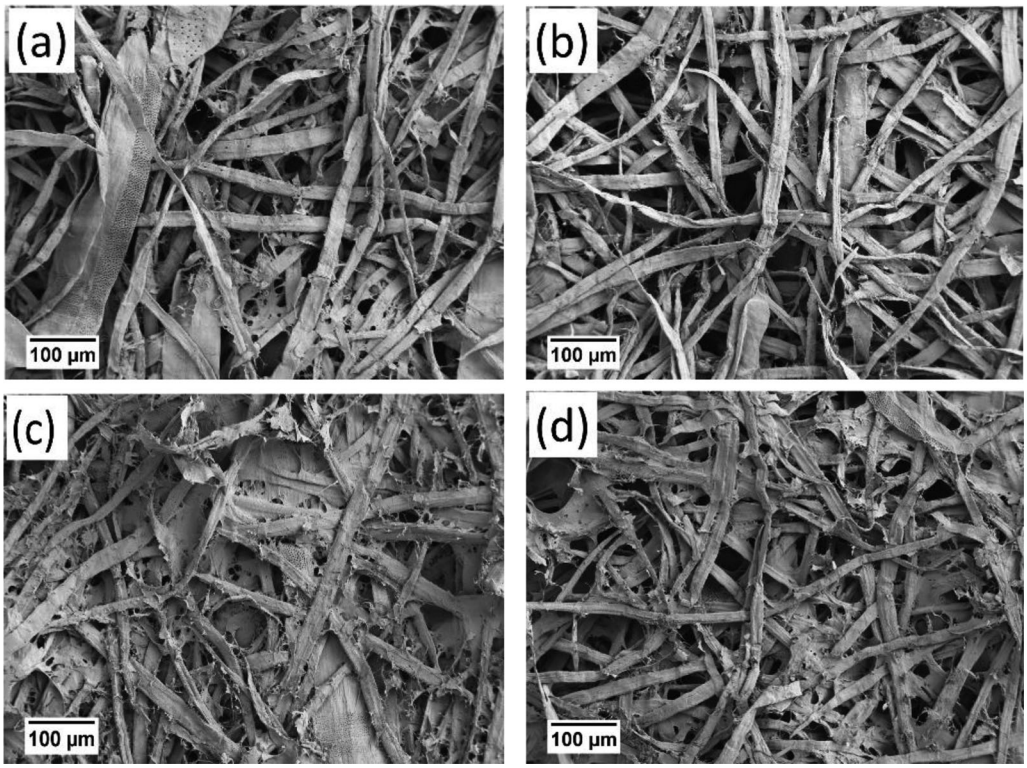

Figure 10. SEM images of a wire side of freeze-dried sheets of (a) P-MNFC0% without bubbles. (b) P-MNFC0% with bubbles. (c) P-MNFC15% without bubbles and (d) P-MNFC15% with bubbles. Images on the left side are without bubbles and on the right with bubbles.

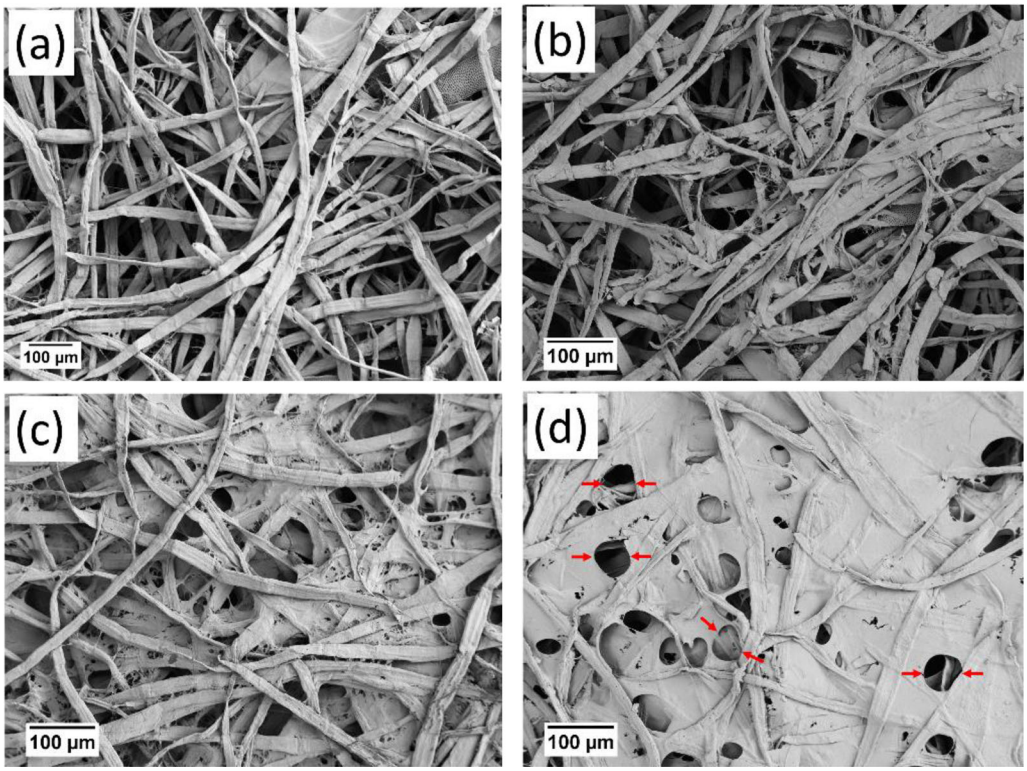

Figure 11. SEM images of a top side of freeze-dried sheets of (a) P-MNFC0% without bubbles. (b) P-MNFC0% with bubbles. (c) P-MNFC15% without bubbles. (d) P-MNFC15% with bubbles.

Table 4. Permeability and apparent density of the freeze-dried sheets.

	Permeability (ml/min.cm^2)		Apparent Density (g/cm^3)	
Samples	Without bubble	With bubble	Without bubble	With bubble
P-MNFC0%	>700	>700	0.227 ± 0.003	0.207 ± 0.002
P-MNFC5%	699 ± 13	>700	0.227 ± 0.002	0.204 ± 0.002
P-MNFC10%	667 ± 26	>700	0.212 ± 0.003	0.202 ± 0.001
P-MNFC15%	210 ± 21	657 ± 10	0.257 ± 0.008	0.196 ± 0.006
P-MNFC20%	130 ± 20	627 ± 38	0.237 ± 0.003	0.162 ± 0.016
P-MNFC25%	N/A	560 ± 60	N/A	0.141 ± 0.010

Table 5. Roughness and specific formation of the freeze-dried sheets.

	Top side roughness proportion (%) [±5μm]		Specific formation ($\sqrt{g}$/m)	
Samples	Without bubble	With bubble	Without bubble	With bubble
P-MNFC0%	12.0 ± 0.3	10.5 ± 0.4	1.10 ± 0.07	0.77 ± 0.16
P-MNFC5%	13.9 ± 0.2	10.9 ± 0.7	0.88 ± 0.06	0.88 ± 0.11
P-MNFC10%	13.0 ± 0.1	12.7 ± 0.7	0.88 ± 0.06	0.76 ± 0.05
P-MNFC15%	14.9 ± 0.5	11.3 ± 1.1	0.81 ± 0.01	0.66 ± 0.04
P-MNFC20%	14.1 ± 0.2	8.1 ± 1.3	0.82 ± 0.01	0.62 ± 0.01
P-MNFC25%	N/A	4.5 ± 0.2	N/A	0.61 ± 0.02

MNFC preferentially adheres to the cationic bubbles which then enrich to the top layer in flotation. With further refinement, this may potentially give a means for producing multilayered structures with applications in e.g., packaging board. A very interesting point is the imprint of micro bubbles with sizes between 50 μm and 100μm in the MNFC layer (Figure 11d, the red arrows). This suggests that one mechanism by which cationic bubbles improve dewatering is by interfering in the natural film forming tendency of MNFC in consolidation.

Analysis of the freeze-dried sheets, shown in Table 4, shed some more light on the dewatering mechanism. The permeability of sheets decreases with increasing MNFC content because MNFC plugs the pores between the fibers. The cationic bubbles have a profound increase in sheet permeability. These results agree with Figure 6 where it can be seen that furnishes with cationic bubbles have a much lower end vacuum. The end vacuum decreases when permeability is higher, and more air can penetrate through the sheet. There are likely several mechanisms at play. The surfactant itself adsorbs onto fiber surfaces and interferes with the development of hydrogen bonds in consolidation, leading to sheets with lower density. This "debonding" effect reduces sheet density and increases permeability. In addition, it is thought that the bubbles help organize the fiber structures into a lower density network, which again will reduce sheet permeability.[40] At 0% and 5% MNFC content, the permeability values were out of range of Bendtsen device which is from 300 to 3500 ml/min.

Scanning surface profilometry was used to characterize the topography of the sheets. In this method, a reference height is defined based on which roughness height is measured.[58] Table 5 shows that when bubbles are used, the top side roughness increases while in the case without bubbles, the top side roughness is nearly independent of MNFC content. The cationic bubbles help distribute the MNFC to the top side where it can fill in the interfiber voids and reduce surface roughness. These results are in agreement with the SEM analysis in Figure 11d.

In Table 5, it can be seen that MNFC also improves the sheet formation. This is because MNFC particles are comparatively short compared to pulp fibers and give less mechanical entanglement and more even mass distribution after dewatering. When bubbles are used, the formation improves further. It is thought that bubbles help to evenly structure the fibrous elements in the suspension and thus improve formation.[40] The cationic bubbles give a pathway to improve dewatering, formation and retention simultaneously. This is not easy to achieve in conventional papermaking.

Conclusion

Addition of cationic bubbles to a nanocellulose rich fiber suspension forms a multifunction system that can improve dewatering, retention and formation simultaneously. The bubbles allow one to increase the amount of MNFC up to 25%, thus increasing the operation window of MNFC application. For example, complete dewatering of a suspension with 25% MNFC was achieved under 5 sec whilst without bubbles, incomplete dewatering is observed with 200 ml furnish remaining.

The important mechanisms for improving the dewatering behavior of cellulosic materials were found to

be solids separation, elevated consistency of separated layer, more even solids distribution, interruption of sheet sealing, debonding and structuring of fibers by the bubbles. This forming method could potentially find use for production of high nanocellulose content papers in a range of packaging and specialty applications.

Acknowledgments

This research was funded by Jane and Aatos Erkko foundation. This work made use of Aalto University Bioeconomy Facilities. The SEM imaging was conducted at Aalto University Nanomicroscopy Centre (Aalto-NMC).

Disclosure of interest statement

The authors report no conflicts of interest. The authors alone are responsible for the content and writing of the paper.

Funding

This work was funded by Jane ja Aatos Erkon Säätiö; Puunjalostusinsinööritry – Forest Products Engineers.

References

[1] Rantanen, J.; Maloney, T. C. Consolidation and Dewatering of a Microfibrillated Cellulose Fiber Composite Paper in Wet Pressing. *Eur. Polym. J.* **2015**, *68*, 585–591. DOI: 10.1016/j.eurpolymj.2015.03.045.

[2] Paulapuro, H. *Papermaking: Stock Preparation and Wet End*; Tappi Pr.: Helsinki, Finland, **2000**.

[3] Sjöstrand, B. Dewatering Aspects at the Forming Section of the Paper Machine. Rewetting and Forming. Fabric Structure. Doctoral dissertation, Karlstads University, Stockholm, Sweden, **2017**.

[4] Rantanen, J. J.; Dimic-Misic, K.; Pirttiniemi, J.; Kuosmanen, P.; Maloney, T. C. Forming and Dewatering of a Microfibrillated Cellulose Composite Paper. *BioResources* **2015**, *10*, 3492–3506. DOI: 10.15376/biores.10.2.3492-3506.

[5] Boufi, S.; Gonzalez, I.; Delgado-Aguilar, M.; Tarres, Q.; Pèlach, M. À.; Mutje, P. Nanofibrillated Cellulose as an Additive in Papermaking Process: A Review. Carbohydr. Polym. **2016**, *154*, 151–166. DOI: 10.1016/j.carbpol.2016.07.117.

[6] Taipale, T.; Ãsterberg, M.; Nykãnen, A.; Ruokolainen, J.; Laine, J. Effect of Microfibrillated Cellulose and Fines on the Drainage of Kraft Pulp Suspension and Paper Strength. *Cellulose* **2010**, *17*, 1005–1020. DOI: 10.1007/s10570-010-9431-9.

[7] Sjöstrand, B.; Barbier, C.; Ullsten, H.; Nilsson, L. Dewatering of Softwood Kraft Pulp with Additives of Microfibrillated Cellulose and Dialcohol Cellulose. *BioResources* **2019**, *14*, 6370–6383.

[8] Turbak, A. F.; Snyder, F. W.; Sandberg, K. R. Microfibrillated Cellulose, a New Cellulose Product: Properties, Uses, and Commercial Potential. J. Appl. Polym. Sci.: Appl. Polym. Symp. (United States) **1983**, 37, 815–827.

[9] Attwood, B. W. A Study of Vacuum Box Operation. *Pap. Technol.* **1962**, *3*, 446–455.

[10] Åslund, P.; Vomhoff, H. Dewatering Mechanisms and Their Influence on Suction Box Dewatering Processes – A Literature Review. *Nord. Pulp Pap. Res. J.* **2008**, *23*, 389–397.

[11] Baldwin, L. High Vacuum Dewatering. *Pap. Technol.* **1997**, *38*, 23–28.

[12] Nordman, L. Laboratory Investigation of Water Removal by a Dynamic Suction Box. *Tappi* **1954**, *37*, 553–580.

[13] Åslund, P.; Vomhoff, H.; Waljanson, A. The Deformation of Chemical and Mechanical Pulp Webs during Suction Box Dewatering. *Nord. Pulp Pap. Res. J.* **2008**, *23*, 403–408.

[14] Ramaswamy, S. Vacuum Dewatering during Paper Manufacturing. *Dry. Technol.* **2003**, *21*, 685–717. DOI: 10.1081/DRT-120019058.

[15] Montgomery, J.; Green, S. I.; Vanerek, A. Paper Physics: Effect of Applied Vacuum Box Suction on Overall Retention in Hand Sheet Forming. *Nord. Pulp Pap. Res. J.* **2010**, *25*, 463–472.

[16] Nilsson, L. Air Flow and Compression Work in Vacuum Dewatering of Paper. *Dry. Technol.* **2014**, *32*, 39–46. DOI: 10.1080/07373937.2013.809732.

[17] Nilsson, L. Stepwise Development of a Mathematical Model for Air Flow in Vacuum Dewatering of Paper. *Dry. Technol.* **2014**, *32*, 1587–1597. DOI: 10.1080/07373937.2014.909844.

[18] Pujara, J.; Siddiqui, M. A.; Liu, Z.; Bjegovic, P.; Takagaki, S. S.; Li, P. Y.; Ramaswamy, S. Method to Characterize the Air Flow and Water Removal Characteristics during Vacuum Dewatering. Part II - Analysis and Characterization. *Dry. Technol.* **2008**, *26*, 341–348. DOI: 10.1080/07373930801898125.

[19] Räisänen, K. High-Vacuum Dewatering on a Paper Machine Wire Section: A Literature Review. *Pap. Ja Puu* **1996**, *78*, 113–120.

[20] Pires, E. C.; Springer, A. M.; Kumar, V. A New Technique for Specific Filtration Resistance Measurement. *Tappi J.* **1989**, *72*, 149–154.

[21] Wildfong, V. J.; Genco, J. M.; Shands, J. A.; Bousfield, D. W. Filtration Mechanics of Sheet Forming. Part I: Apparatus for Determination of Constant-Pressure Filtration Resistance. *J. Pulp Pap. Sci.* **2000**, *26*, 250–254.

[22] Räisänen, K. O.; Paulapuro, H.; Karrila, S. Wire Section Simulation with the Moving Belt Drainage Tester (MBDT). In *Papermakers Conference*; TAPPI Press, Atlanta, USA, April, **1993**; p 103–133.

[23] Hubbe, M. A.; Heitmann, J. A. Review of Factors Affecting the Release of Water from Cellulosic Fibers during Paper Manufacture. *BioResources* **2007**, *2*, 500–533.

[24] Hubbe, M.; Sjöstrand, B.; Nilsson, L.; Koponen, A. I.; McDonald, D. Rate-Limiting Mechanisms of Water Removal during the Formation, Vacuum Dewatering, and Wet-Pressing of Paper Webs: A Review. *BioResources* 2020, *15* (4), 9672–9755.
[25] Horn, D.; Melzer, J. Influence of High-Molecular Cationic Dehydration Agents on Electrokinetic Properties of Pulp. *Papier* **1975**, *29*, 534–541.
[26] Gruber, E.; Grossmann, K.; Schempp, W. Interactions of Synthetic Cationic Polymers with Fibres and Fillers. 1. *Wochenblatt FUR Pap.* **1996**, *124*, 4.
[27] Pruden, B. The effect of fines on paper properties. *Pap. Technol.* **2005**, *46*, 19–26.
[28] Mörseburg, K.; Chinga-Carrasco, G. Assessing the Combined Benefits of Clay and Nanofibrillated Cellulose in Layered TMP-Based Sheets. *Cellulose* **2009**, *16*, 795–806. DOI: 10.1007/s10570-009-9290-4.
[29] Korhonen, M. Flocculation/Deflocculation of Cellulosic Materials and Mineral Particles by Polyelectrolyte Complexes and Nanocelluloses. Doctoral dissertation, Aalto University, Espoo, Finland, **2015**.
[30] Maloney, T. C. Network Swelling of TEMPO-Oxidized Nanocellulose. *Holzforschung* **2015**, *69*, 207–213. DOI: 10.1515/hf-2014-0013.
[31] Merayo, N.; Balea, A.; de la Fuente, E.; Blanco, Á.; Negro, C. Synergies between Cellulose Nanofibers and Retention Additives to Improve Recycled Paper Properties and the Drainage Process. *Cellulose* **2017**, *24*, 2987–3000. DOI: 10.1007/s10570-017-1302-1.
[32] Sim, K.; Lee, J.; Lee, H.; Youn, H. J. Flocculation Behavior of Cellulose Nanofibrils under Different Salt Conditions and Its Impact on Network Strength and Dewatering Ability. *Cellulose* **2015**, *22*, 3689–3700. DOI: 10.1007/s10570-015-0784-y.
[33] Chen, L. C.; Chien, C. Y.; Chu, C. P.; Lee, D. J.; Hsieh, K. H.; Lee, C. H.; Liu, J. C. Conditioning and Dewatering of Pulp and Paper Sludge. *Dry. Technol.* **2002**, *20*, 967–988. DOI: 10.1081/DRT-120003772.
[34] Dimic-Misic, K.; Puisto, A.; Paltakari, J.; Alava, M.; Maloney, T. The Influence of Shear on the Dewatering of High Consistency Nanofibrillated Cellulose Furnishes. *Cellulose* **2013**, *20*, 1853–1864. DOI: 10.1007/s10570-013-9964-9.
[35] Dimic-Misic, K.; Puisto, A.; Gane, P.; Nieminen, K.; Alava, M.; Paltakari, J.; Maloney, T. The Role of MFC/NFC Swelling in the Rheological Behavior and Dewatering of High Consistency Furnishes. *Cellulose* **2013**, *20*, 2847–2861. DOI: 10.1007/s10570-013-0076-3.
[36] Hakovirta, M.; Aksoy, B.; Nichols, O.; Farag, R.; Ashurst, W. R. Functionalized Cellulose Fibers for Dewatering and Energy Efficiency Improvement. *Dry. Technol.* **2014**, *32*, 1401–1408. DOI: 10.1080/07373937.2014.887576.
[37] Korhonen, M.; Puisto, A.; Alava, M.; Maloney, T. The Effect of Pressure Pulsing on the Mechanical Dewatering of Nanofiber Suspensions. *Chem. Eng. Sci.* **2020**, *212*, 115267. DOI: 10.1016/j.ces.2019.115267.
[38] Wetterling, J.; Sahlin, K.; Mattsson, T.; Westman, G.; Theliander, H. Electroosmotic Dewatering of Cellulose Nanocrystals. *Cellulose* **2018**, *25*, 2321–2329. DOI: 10.1007/s10570-018-1733-3.
[39] Kinnunen, K.; Lehmonen, J.; Beletski, N.; Jetsu, P.; Hjelt, T. Benefits of Foam Forming Technology and Its Applicability in High MFC Addition Structures. In *Proceedings of the 15th Fundamental Research Symposium*. Advances in Pulp and Paper Research. The Pulp & Paper Fundamental Research Society, Cambridge, **2013**, p. 837–850.
[40] Lehmonen, J.; Jetsu, P.; Kinnunen, K.; Hjelt, T. Potential of Foam-Laid Forming Technology in Paper Applications. *Nord. Pulp Pap. Res. J.* **2013**, *28*, 392–398. DOI: 10.3183/npprj-2013-28-03-p392-398.
[41] Timofeev, O.; Jetsu, P.; Kiiskinen, H.; Keränen, J. T. Drying of Foam-Formed Mats from Virgin Pine Fibers. *Dry. Technol.* **2016**, *34*, 1210–1218. DOI: 10.1080/07373937.2015.1103254.
[42] Lehmonen, J.; Retulainen, E.; Paltakari, J.; Kinnunen-Raudaskoski, K.; Koponen, A. Dewatering of Foam-Laid and Water-Laid Structures and the Formed Web Properties. *Cellulose* **2020**, *27*, 1120–1147. DOI: 10.1007/s10570-019-02913-z.
[43] Marui, T. An Introduction to Micro/Nano-Bubbles and Their Applications. *Syst. Cybern. Informatics* **2013**, *11*, 68–73.
[44] Tsuge, H. *Micro-and Nanobubbles: Fundamentals and Applications*; CRC Press: Pan Stanford, USA, **2014**.
[45] Temesgen, T.; Bui, T. T.; Han, M.; Kim, T.; Park, H. Micro and Nanobubble Technologies as a New Horizon for Water-Treatment Techniques: A Review. *Adv Colloid Interface Sci.* **2017**, *246*, 40–51. DOI: 10.1016/j.cis.2017.06.011.
[46] Xu, Q.; Nakajima, M.; Ichikawa, S.; Nakamura, N.; Shiina, T. A Comparative Study of Microbubble Generation by Mechanical Agitation and Sonication. *Innov. Food Sci. Emerg. Technol.* **2008**, *9*, 489–494. DOI: 10.1016/j.ifset.2008.03.003.
[47] Calgaroto, S.; Wilberg, K. Q.; Rubio, J. On the Nanobubbles Interfacial Properties and Future Applications in Flotation. *Miner. Eng.* **2014**, *60*, 33–40. DOI: 10.1016/j.mineng.2014.02.002.
[48] Kim, S.; Kim, H.; Han, M.; Kim, T. Generation of Sub-Micron (Nano) Bubbles and Characterization of Their Fundamental Properties. *Environ. Eng. Res.* **2018**, *24*, 382–388. DOI: 10.4491/eer.2018.210.
[49] Etchepare, R.; Oliveira, H.; Nicknig, M.; Azevedo, A.; Rubio, J. Nanobubbles: Generation Using a Multiphase Pump, Properties and Features in Flotation. *Miner. Eng.* **2017**, *112*, 19–26. DOI: 10.1016/j.mineng.2017.06.020.
[50] Calgaroto, S.; Azevedo, A.; Rubio, J. Flotation of Quartz Particles Assisted by Nanobubbles. *Int. J. Miner. Process* **2015**, *137*, 64–70. DOI: 10.1016/j.minpro.2015.02.010.
[51] Calgaroto, S.; Azevedo, A.; Rubio, J. Separation of Amine-Insoluble Species by Flotation with Nano and Microbubbles. *Miner. Eng.* **2016**, *89*, 24–29. DOI: 10.1016/j.mineng.2016.01.006.
[52] Höke, U., & Schabel, S. *Recycled Fibre and Deinking*; Paper Engineers' Association/Paperi ja Puu Oy, Helsinki, Finland, **2009**.

[53] Kangas, H.; Lahtinen, P.; Sneck, A.; Saariaho, A.-M.; Laitinen, O.; Hellen, E. Characterization of Fibrillated Celluloses. A Short Review and Evaluation of Characteristics with a Combination of Methods. *Nord. Pulp Pap. Res. J.* **2014**, *29*, 129–143. DOI: 10.3183/npprj-2014-29-01-p129-143.

[54] Koponen, A.; Haavisto, S.; Liukkonen, J.; Salmela, J. Analysis of the Effects of Pressure Profile, Furnish, and Microfibrillated Cellulose on the Dewatering of Papermaking Furnishes. *TJ* **2015**, *14*, 325–337. DOI: 10.32964/TJ14.5.325.

[55] Britt, K. W.; Unbehend, J. E. Water Removal during Paper Formation. *Tappi J.* **1985**, *68*, 104–107.

[56] Dong, C.; Song, D.; Patterson, T.; Ragauskas, A.; Deng, Y. Energy Saving in Papermaking through Filler Addition. *Ind. Eng. Chem. Res.* **2008**, *47*, 8430–8435. DOI: 10.1021/ie8011159.

[57] Cameron, A. C.; Windmeijer, F. A. G. An R-Squared Measure of Goodness of Fit for Some Common Nonlinear Regression Models. *J. Econ.* **1997**, *77*, 329–342. DOI: 10.1016/S0304-4076(96)01818-0.

[58] Niskanen, K. *Paper Physics*; Papermaking Science and Technology: A Series of 19 Books; Finnish Paper Engineer's Association/Paperi ja Puu Oy, Helsinki, Finland, **2008**.

[59] Zhang, L.; Batchelor, W.; Varanasi, S.; Tsuzuki, T.; Wang, X. Effect of Cellulose Nanofiber Dimensions on Sheet Forming through Filtration. *Cellulose* **2012**, *19*, 561–574. DOI: 10.1007/s10570-011-9641-9.